Proceedings of the 2006 IASME/WSEAS International Conference on Energy & Environmental Systems, Chalkida, Greece, May 8-10, 2006 (pp43-48)

Numerical prediction of the flow field produced by a laboratory-scale combustor: a preliminary isothermal investigation

[1*]A. HATZIAPOSTOLOU, [2]K. KRALLIS, [2]N.G. ORFANOUDAKIS, [2]M.K. KOUKOU,
[3]D. CHATZIFOTIS, [1]G. RAPTIS
[1]Energy Technology Dept., TEI of Athens, Ag. Spyridonos str., 12210, Athens, GREECE
[2]Mechanical Engineering Dept., TEI of Chalkida, 344 00 Psachna, Evia GREECE
[3]PPC, Thermal Power Plants Division, Chalkokondili 30, 10432, Athens, GREECE

Abstract: - A multi-fuel swirl-stabilized laboratory burner of 100kW total thermal input has been developed, designed as a scale model of a 110MW coal burner. In this research, a Computational Fluid Dynamics (CFD) work was performed in order to assess swirl and axial velocities for the burner isothermal application. The predictions were compared with measured quantities in terms of flow field at various distances away from the burner exit. It is confirmed that the RNG k-ε and the Realizable k-ε turbulence models produce more accurate results than the standard k-ε model while the RNG k-ε model has a small advantage over the Realizable k-ε model, within the range of swirl number involved.

Key-Words: - combustor, laboratory-scale, simulation

1 Introduction

Pollutant emissions reduction and flame stabilization are among the major problems in combined cycle power plants and conventional power plants. Because of the recent European Directives it is a common concern for combustor manufacturers and plant operators to achieve improvement of the environmental effects of the plants without a significant decrease in their efficiency [1-3]. Due to the growing awareness concerning combustion related pollutant emissions and global warming, there is an increasing need towards optimization of these systems. An important way of understanding flame processes is to scale-up the measurements' results of tests on small burners to larger ones. Ideally, the result of a burner and flame scaling would be the complete similarity of all the combustion processes (turbulent transport and mixing, heat generation, heat transfer) in the scale down domain. However, that is not feasible, as all the physical and chemical processes will not scale down in the same way.

Towards the above issues, a multi-fuel swirl-stabilized laboratory burner of 100kW total thermal input has been developed, designed as a scale model of a 110MW coal burner. Constant velocity scaling criterion was applied to retain similarity to the industrial burner. Swirling flows are used as means of controlling flames in combustion chambers and have also found application in various types of burners in order to achieve the desired ignition and burnout characteristics for a given fuel. The burner is able to produce flames with different aerodynamic characteristics, and to burn a combination of gaseous, liquid and pulverized solid fuels. In this context, the conditions for safe combustion of a combination of fuels in terms of flame stabilization, sufficient combustion efficiency and reduced pollutants emissions can be studied. The measurements provide further understanding on how swirl interacts with the combustion process occurring in this type of industrial burners and can lead to conclusions about the behavior of coal particles or droplets within the flame, as well as the emission production.

To enhance understanding on the effect of the swirl number on the fluid motion, the non-combusting flow field downstream the burner was investigated by the use of CFD techniques. Results are reported as a function of swirl number and compared to experimental data obtained in the same burner in the absence of combustion.

2 Problem Formulation

2.1 The laboratory burner

Fig. 1 depicts the installation of the laboratory burner. The laboratory burner, which is shown schematically in Figs. 2a and b, was designed as a scale model of an industrial coal burner operating in a cement rotary kiln. It can burn a mixture of liquid, gaseous and pulverized solid fuel simultaneously (if required) and produce flows with different degrees of swirl. Another basic design criterion was the similarity to the real industrial burner, which was accomplished by employing the constant velocity (CV) scaling criterion mentioned in [4]. The burner

consists of a cylindrical body for the secondary airflow with a central fuel pipe. The exit of the burner is at the top of the burner and the diameter of the inner wall of the outer tube (shown as D_e) is known as the burner exit diameter.

Fig. 1. Rotameters, air pipelines, combustor and solid fuel kit.

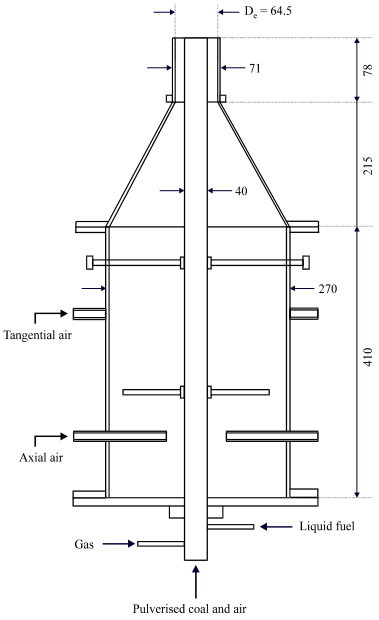

Fig. 2. Schematic of the laboratory burner (a) with enlarged view of the fuel gun (b).

The latter is a characteristic dimension for every burner and in this case is D_e=64.5 mm. Secondary air is divided in swirl and axial air. The swirl air is introduced tangentially from four entries located symmetrically around the burner. The axial air is introduced vertically to the outer wall of the burner, from four entries located also symmetrically and below the tangential entries. Inside the burner there is a plate located between the entries of axial and swirl air in order to achieve more homogeneous axial flow. The axial flow has only axial velocity and the swirl flow has axial and tangential velocity component (swirl component). At the upper part of the burner the outer cylinder wall contracts to produce a homogeneous symmetrical secondary airflow at the burner exit. The central fuel pipe consists of three individually sealed coaxial tubes. The inner tube is for the liquid fuel, the annular area between the inner and the middle tube is for the pulverised coal and the annular area between the outer and the middle tube is for the gas fuel (Fig. 2.b). The liquid fuel is dispersed at the end of the tube by an atomising nozzle. The pulverised coal is pneumatically conveyed by an airflow and is axially injected into the gas fuel flame as primary air/coal flow. The gas fuel is injected radially through two rows of 20 holes of 1mm diameter around the outer tube. The amount of swirl in the flow can be adjusted by varying the ratio of axial and tangential air, while maintaining the same total air flow rate.

2.2 Mathematical model

2.2.1 Geometry and Computational mesh

The simulations were performed for a flow domain that extended from the burner exit upwards at a distance of $30D_e$ and radially outwards at $10D_e$.

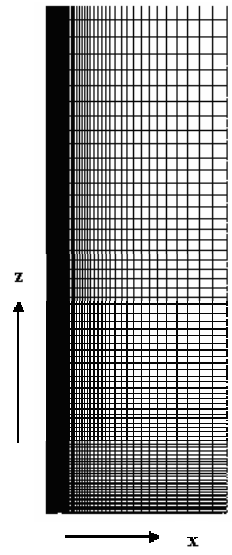

Fig. 3 View of the 2D mesh used in the simulations. The axis of symmetry z is on the left-hand side.

The domain started from an axial distance of 4.5mm away from the burner exit, since that was the nearest position where velocity measurements were taken. Since the geometry is axisymmetric, the mesh

covered half the domain to be solved. A number of meshes with different densities were constructed in order to test the sensitivity of the solution. The mesh shown in Figure 3 was finally selected to be used in all simulations and was consisted of 5175 cells.

2.2.2 Governing Equations - Boundary conditions

The turbulent flow field downstream the burner, was calculated from the solution of the two-dimensional, isothermal, axisymmetric, steady-state, Reynolds-averaged Navier-Stokes equations by use of the commercially available code Fluent®. Air was utilized as the background fluid. Boundary conditions were imposed from the experimentally measured velocity profiles of the axial and swirl velocity components at $z/D_e = 0.045$ and a total of three cases corresponding to low (S_w=0.45), medium (S_w=0.65) and high (S_w=0.9) swirl were considered.

2.2.3 Turbulence modeling

The Reynolds stresses which appear as unknowns in the Reynolds averaged forms of the Navier-Stokes equations for the velocity components were modeled by use of three turbulence models available in the Fluent® code: the standard k-ε model, the RNG k-ε model, based on the so-called "renormalization group theory", and the Realizable k-ε model. The standard two-equation k-ε turbulence model involves the solution of two additional partial differential equations for the turbulent kinetic energy (k) and its dissipation rate (ε) [7,8]. The values of the constants C_μ, C_1, C_2, σ_κ and σ_ε applied are 0.09, 1.44, 1.92, 1.0 and 1.3 respectively [7,8]. The RNG k-ε model is essentially a variation of the standard k-ε model, with the used constants estimated rather through a statistical mechanics approach than from experimental data. The values of the constants C_μ, C_1 and C_2 applied are 0.0845, 1.42 and 1.68, respectively [9]. For the Realizable k-ε model the term "realizable" means that the model satisfies certain mathematical constraints on the Reynolds stresses, consistent with the physics of turbulent flows. The Realizable k-ε model contains a new formulation for the turbulent viscosity. Also, a new transport equation for the dissipation rate, ε, has been derived from an exact equation for the transport of the mean-square vorticity fluctuation [10]. Both the Realizable and RNG k-ε models have shown substantial improvements over the standard k-ε model where the flow features include strong streamline curvature, vortices and rotation. Since the last model is still relatively new, it is not clear in exactly which instances the Realizable k-ε model consistently outperforms the RNG model. The accuracy of the predictions of these models was checked against the measured flow field (swirl and axial velocities).

2.2.4 Numerical solution details

The solution of the set of the equations has been made with the segregated steady-state solver [10] embodied in the Fluent® commercial software. The convergence is checked by several criteria (e.g. the conservation equations should be balanced; the residuals of the discretised conservation equations must steadily decrease).

3 Results and Discussion

Fig. 4 presents profiles of the mean axial velocity component along the burner centreline as a function of the swirl number. These profiles show the extent of the recirculation zone (IRZ) on the centerline, which, as expected is larger in the case of the high swirl number flow case. In all three cases, it is evident that the standard k-ε model tends to underestimate the magnitude of the measured axial velocity component and the size of the internal recirculation zone (IRZ). Results obtained with both the RNG and Realizable k-ε models are generally in good agreement with the measurements, with few deviations in certain areas. At S_w = 0.45 and 0.65, all models fail to predict the positive mean axial velocity magnitude in the area very close to the burner exit (Fig. 4a and b). However, the two most advanced turbulence models are successful in predicting the general trend in all profiles, with the RNG k-ε model having a small advantage over the Realizable k-ε model. The radial variations of the axial and swirl velocity components at two axial locations close to the burner exit (at z/De=0.78 or 0.62, Figs. 5 & 6) and far from the burner exit (z/De=2 or 2.32, Figs. 7 & 8) for all three swirl numbers are shown in the subsequent figures for all turbulence models. All radial profiles shown are halves, with the axis of symmetry at x=0. The radial velocity components were also measured, but they are not shown, as their magnitude is considerably smaller and, most importantly, their radial profiles tend to strongly deviate from the axial symmetry, possibly due to minor burner structural asymmetries. Close to the burner exit, all models predict quite accurately the mean swirl velocity component (Fig. 5), especially at the two lower swirl numbers. At the same locations, the axial velocity radial profiles (Fig. 6) are better predicted by the RNG k-ε model, followed by the Realizable k-ε model. The prediction accuracy also varies with the swirl number: at the high swirl number cases (especially at the S_w=0.65 flow case), the agreement between

measured data and the RNG model-computed data is remarkable, whereas at the low swirl number case (S_w=0.45), a deviation can be seen. However, the RNG model still offers a better option as turbulence model.

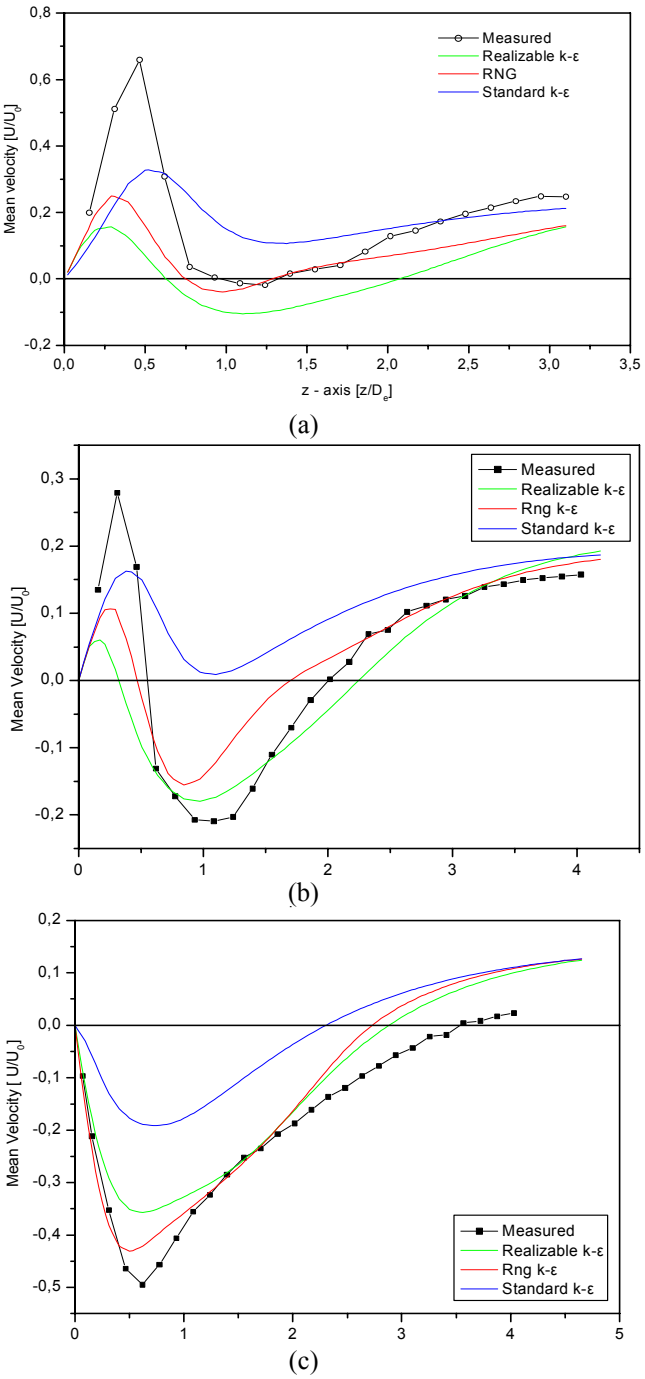

Fig. 4. Mean axial velocity profiles along the burner centerline for the three flow cases (a) S_w=0.45 (b) S_w=0.65 and (c) S_w=0.90

The standard k-ε model clearly fails to predict the negative axial velocities and this is more pronounced in the high swirl case. Further downstream (z/De=2 to 2.32), predictions tend to produce slightly worst results.

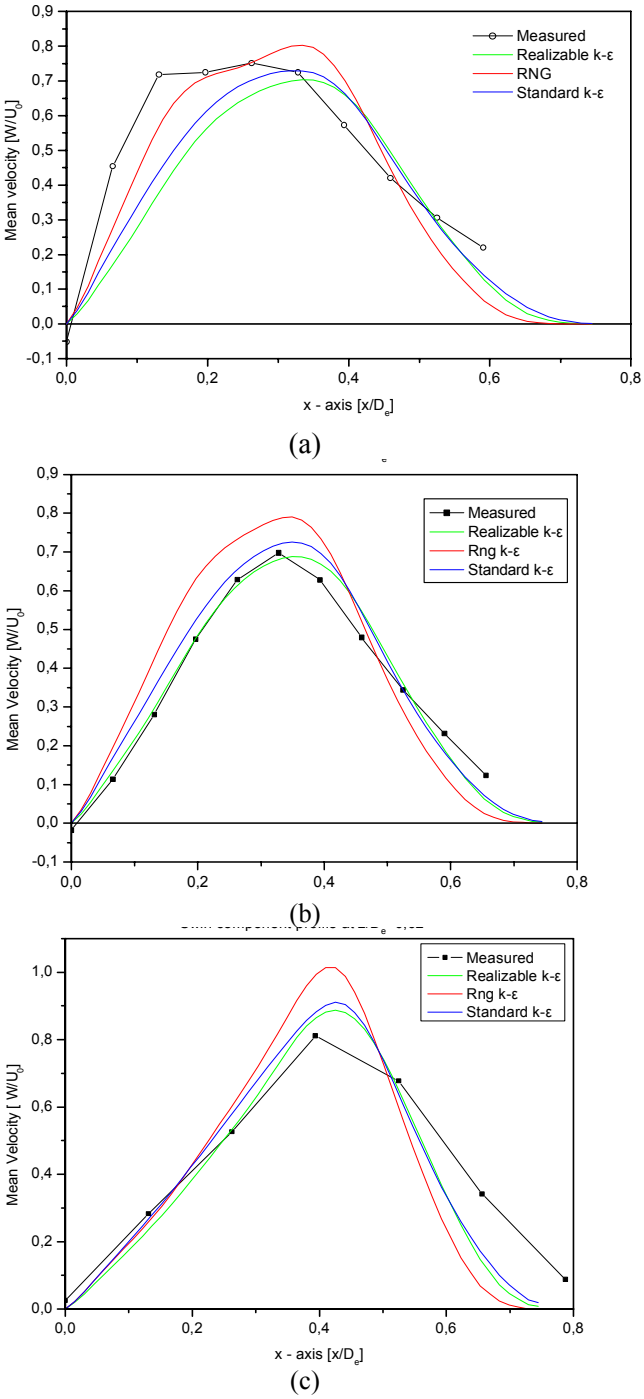

Fig. 5. Radial (half) profiles of the mean swirl velocity component for the three flow cases (a) S_w=0.45 at z/De=0.78 (b) S_w=0.65 at z/De=0.78 and (c) S_w=0.90 at z/De=0.62

The comparisons concerning the radial half profiles of the swirl mean velocity component at all swirl number cases (Fig. 7) show that there is an overestimation of the swirl component magnitude by all models used, especially in the case of the RNG k-ε model. At these locations, the Realizable k-ε model seems to produce more accurate results in comparison with the RNG k-ε model.

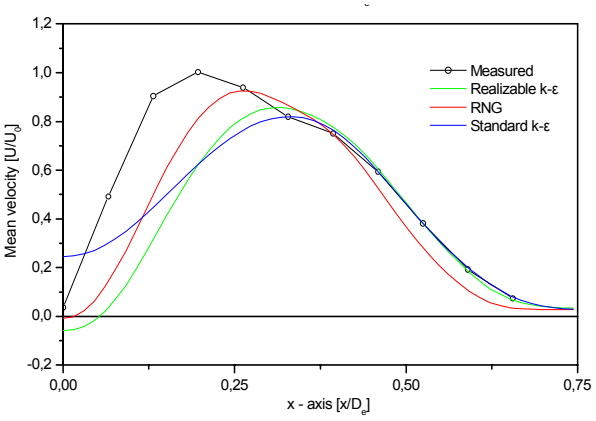

(a)

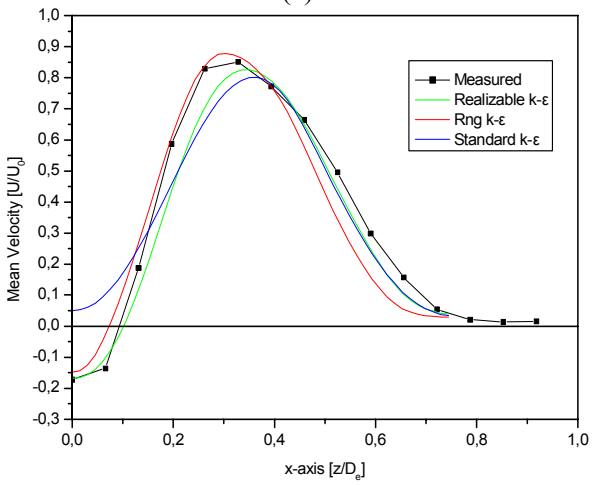

(b)

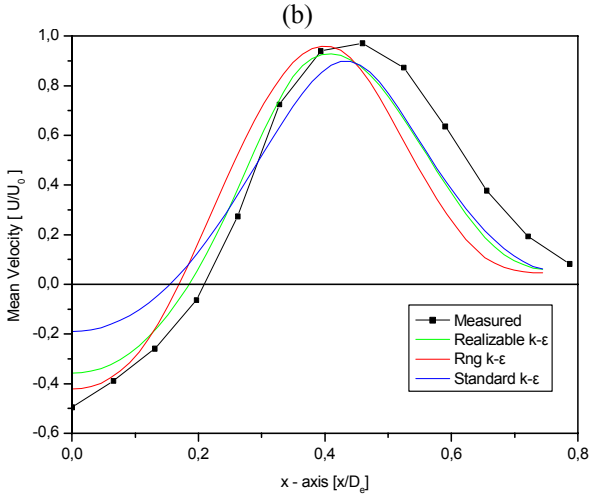

(c)

Fig. 6. Radial (half) profiles of the mean axial velocity component for the three flow cases (a) S_w=0.45 at z/De=0.78 (b) S_w=0.65 at z/De=0.78 and (c) S_w=0.90 at z/De=0.62

Finally the axial velocity component comparisons (Fig. 8) show that the agreement between measured data and predictions is satisfactory, especially at the two higher swirl number cases.

Taking into account the comparisons between measured data and predicted velocity magnitudes at all locations, by means of all models, it is confirmed that the two more advanced turbulence models produce more accurate results than the standard k-ε model.

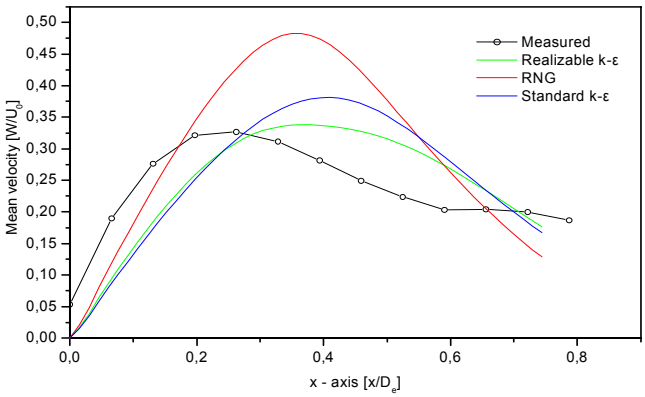

(a)

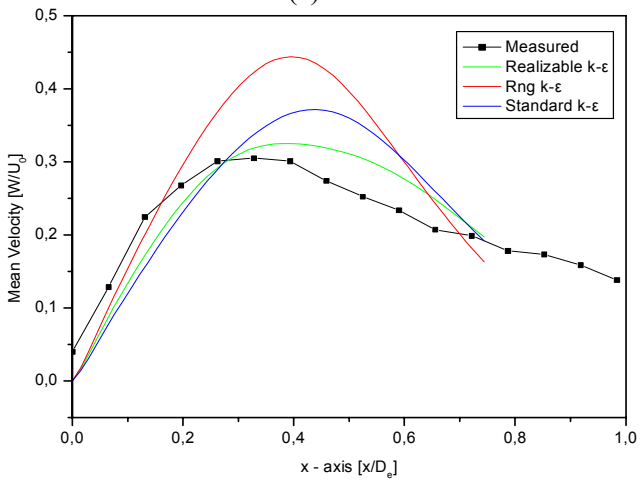

(b)

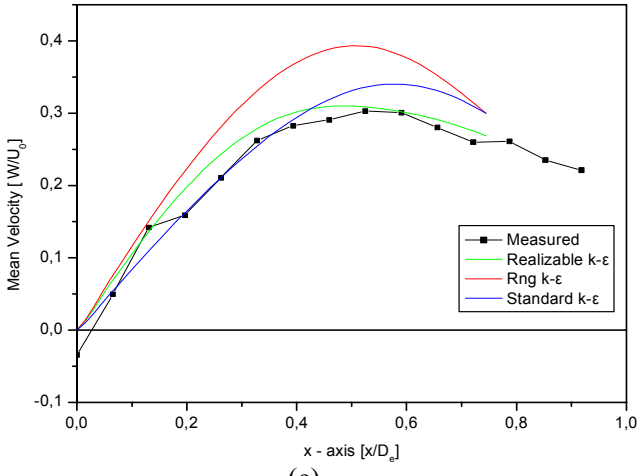

(c)

Fig. 7. Radial (half) profiles of the mean swirl velocity component for the three flow cases (a) S_w=0.45 at z/De=2 (b) S_w=0.65 at z/De=2 and (c) S_w=0.90 at z/De=2.32

It is not entirely clear, which one of the two advanced models is better in these strongly swirling flows. After careful consideration of all data available, it can be concluded that the RNG k-ε

model has a small advantage over the Realizable k-ε model, within the range of swirl number involved.

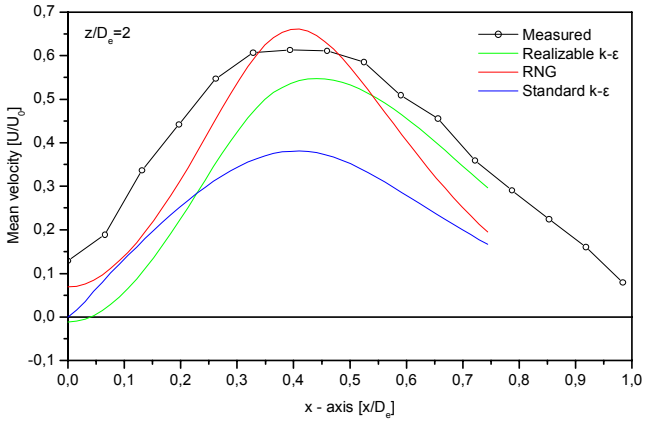

(a)

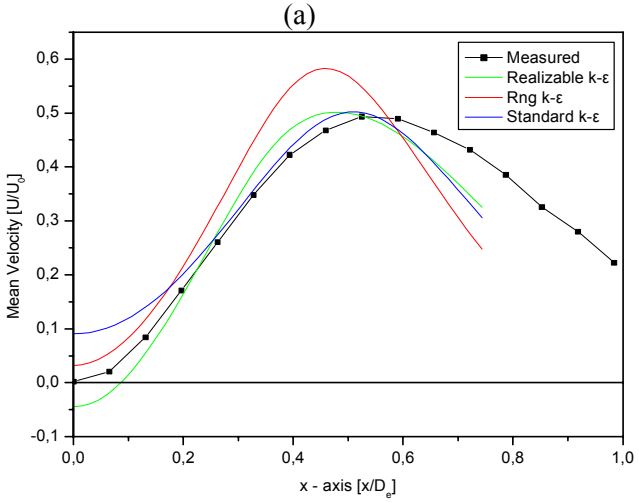

(b)

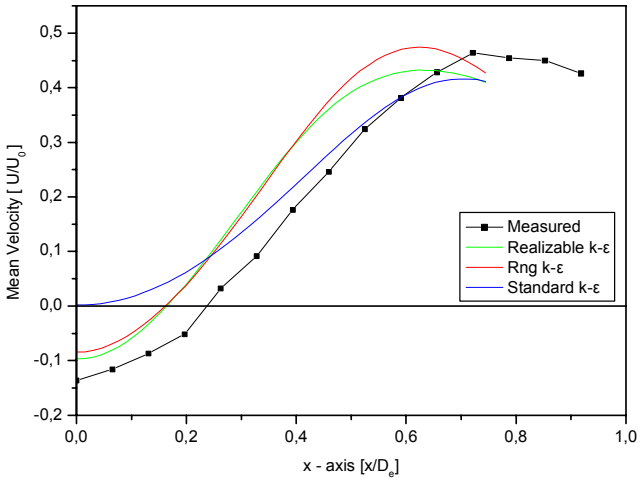

(c)

Fig. 8. Radial (half) profiles of the mean axial velocity component for the three flow cases (a) S_w=0.45 at z/De=2 (b) S_w=0.65 at z/De=2 and (c) S_w=0.90 at z/De=2.32

4 Conclusion

A Computational Fluid Dynamics (CFD) work was performed in order to assess swirl and axial velocities for a burner isothermal application. The predictions were compared with measured quantities in terms of flow field at various distances away from the burner exit. It is confirmed that the RNG k-ε and the Realizable k-ε turbulence models produce more accurate results than the standard k-ε model while the RNG k-ε model has a small advantage over the Realizable k-ε model, within the range of swirl number involved.

5 Acknowledgement

Authors would like to thank Hellenic Ministry of National Education and Religious Affairs and European Commission that financially supported this work under the auspices of the Operational Programme for Education and Initial Vocational Training, Archimedes I and II Programme.

References:

[1]N.G. Orfanoudakis, K. Krallis, A. Hatziapostolou, A. Vakalis, N.W. Vlachakis, Emission Reduction Techniques: the IPPC EC Directive, Air Pollution 2004, Rhodes GREECE, WIT Press.

[2]W. Kaewboonsong, V.I. Kouprianov, Minimizing fuel and "external" costs for a variable-load utility boiler firing fuel oil", *Int. Journal of Thermal Sciences*, Vol. 42, 2004, pp. 889-895.

[3]G.L. Borman, K.W. Ragland, *Combustion Engineering*, Mc Graw Hill, New York, 1998.

[4]J.P. Smart, D..J. Morgan, The comparison between constant velocity and constant residence time scaling of the aerodynamically air staged burner, Netherlands: International Flame Research Foundation Doc No F37/y/28, 1992.

[5]N.G. Orfanoudakis, Measurements of size and velocity of burning coal, PhD Thesis, Imperial College of Science, Technology and Medicine, Department of Mechanical Engineering, 1994.

[6]A. Hatziapostolou, Swirling flows in direct-injection diesel engines, PhD Thesis, Imperial College of Science, Technology and Medicine, Department of Mechanical Engineering, 1991.

[7] B.E. Launder, D.B. Spalding, The Numerical Computation of Turbulent Flow, *Computer Methods in Applied Mechanics and Engineering*, Vol. 3, 1974, pp. 269-289.

[8] W. Rodi, *Turbulence models and their application in hydraulics – A state of the art review*, Int. Ass. for Hydraulics Research, 1980.

[9] V. Yakhot, S.A. Orszag, Renormalization group analysis of turbulence. I. Basic theory, *Journal of Scientific Computing*, Vol. 1 (1), 1986, pp. 3-51.

[10] Fluent® User's Guide.